Title: Phosphorylation of Gαi shapes canonical Gα(i)βγ/GPCR signaling

Authors: Suchismita Roy [1], Ananta James Silas[1], Majid Ghassemian[6], Irina Kufareva[4]* and Pradipta Ghosh*[1-3]

Affiliations:

[1]Department of Cellular and Molecular Medicine, University of California San Diego, CA, USA;

[2]Department of Medicine, University of California San Diego, CA, USA;

[3]Moore's Comprehensive Cancer Center, University of California San Diego, CA, USA;

[4]Skaggs School of Pharmacy and Pharmaceutical Sciences, University of California San Diego, CA, USA;

[5]Department of Chemistry and Biochemistry, Biomolecular and Proteomics Mass Spectrometry Facility, University of California San Diego, San Diego, CA, USA.

***Corresponding author:**

*Irina Kufareva, Ph.D.; Associate Adjunct Professor, Skaggs School of Pharmacy and Pharmaceutical Sciences, University of California San Diego, 9500 Gilman Drive, SSPSS Building, Rm 3151, 239; La Jolla, CA 92093. Phone. 858-822-4163 Email: ikufareva@ucsd.edu

*Pradipta Ghosh, M.D.; Professor, Departments of Medicine and Cellular and Molecular Medicine, University of California San Diego; 9500 Gilman Drive (MC 0651), George E. Palade Building, Rm 232, 239; La Jolla, CA 92093. Phone: 858-822-7633. Email: prghosh@ucsd.edu

Abstract (Abstract should not exceed 250 words)

A long-standing question in the field of signal transduction is to understand the interplay between distinct signaling pathways that control cell behavior. For growth factors and heterotrimeric G proteins, the two major signaling hubs in eukaryotes, the mechanisms of independent signal transduction have been extensively characterized; however, if/how they may cross talk remains obscure. Here we use linear-ion-trap mass spectrometry in combination with cell-based biophysical, biochemical, and phenotypic assays to chart at least three distinct ways in which growth factors may impact canonical Gα(i)βγ signaling downstream of a GPCR (CXCR4) via phosphorylation of Gαi. Phosphomimicking mutations in a cluster of residues in the αE helix (Y154/155) result in the suppression of agonist-induced Gα(i) activation while promoting constitutive Gβγ signaling; others in the P-loop (S44, S47, T48) suppress Gi activation entirely thus completely segregating the growth factor and GPCR pathways. While most phosphoevents appear to impact, as expected, the core properties of Gα(i) (conformational stability, nucleotide binding, Gβγ association and release, etc.), one phosphomimicking mutation promoted mislocalization of Gαi from the plasma membrane: a novel and unexpected mechanism of GPCR signal suppression. A phosphomutation of C-terminal Y320 was sufficient to orchestrate such suppression by protein compartmentalization. Findings not only elucidate how growth factor and chemokine signals crosstalk through phosphomodulation of Gαi, but also how such crosstalk may generate signal diversity.

One sentence title: Phosphorylation of Gαi shapes canonical Gi/GPCR signaling

INTRODUCTION

A cell perceives and calibrates its responses to the external cues by a complex array of sensor proteins, commonly known as 'receptors'; these receptors transduce signals from the plasma membrane (PM) to the cell's interior via a cascade of downstream intermediates. Traditionally studied through reductionist approaches by dissecting a single cascade at a time, it is well-known that these distinct cascades crosstalk at multiple levels. Cross-talks between multiple cascades generate complex larger network for information flow, integration and diversification (through context, time and space), all of which ultimately coordinately controls cell fate (1-4).

In eukaryotes, two of the most widely studied signaling cascades are those that are initiated by the receptor tyrosine kinases (RTKs) and by the 7-transmembrane receptors coupled to heterotrimeric G proteins (GPCRs)(5). Upon sensing specific growth factors, RTKs auto-phosphorylate their cytoplasmic tails; subsequently, a variety of adaptor proteins dock onto those phosphosites to propagate the signal to the cell's interior (6). Heterotrimeric (henceforth, trimeric) G proteins, on the other hand, serve as molecular switches, canonically acting downstream of GPCRs (7, 8). Agonist-bound GPCRs act as receptor guanine-nucleotide exchange factors (GEFs) for heterotrimeric G proteins, triggering GDP to GTP exchange on Gα subunit and releasing Gβγ dimers; GTP-bound Gα monomers and Gβγ dimers go on to bind the effector molecules and transduce a variety of signals (7).

Although it has been suggested that these two pathways crosstalk (9-13), in that G proteins may be activated downstream of RTK (14-24), whether and how these processes take place in cells, and their biological significance still remains ambiguous. Reports as early as the late 1980's and early 1990's had suggested that tyrosine phosphorylation of G proteins is one such mechanism (25-28); however, the identity of these sites and how they may impact G protein activity remained unknown until recently when Kalogriopoulos et al. (5) showed that RTKs directly phosphorylate and transactivate the α-subunit of the trimeric Gi protein. Upon growth factor stimulation, scaffolding of monomeric Gαi with RTKs (via a multi-modular signal transducer, GIV/a.k.a Girdin) (29) facilitates the phosphorylation on two tyrosines located within the inter-domain cleft of Gαi. Phosphorylation activates (by enhancing the basal exchange rate) of Gαi and inhibits second messengers (cAMP). These insights defined a tyrosine-based G protein signaling paradigm and revealed its importance in eukaryotes; they also raised at least two important questions—(i) Given the plethora of kinases that are activated upon growth factor stimulation (not just TKs), what other sites may be phosphorylated and how might they (alone or in combination) impact Gαi activation?; and (ii) How might these phosphoevents impact the ability of canonical GPCRs to transduce signals via Gi? Furthermore, although growth factors (EGF and IGF1) were found to inhibit Gi coupling to and activation by GPCRs (CXCR4)(26, 30), mechanisms for such uncoupling/deactivation remain elusive.

Here we tackle these outstanding questions by interrogating how one prototypical growth factor/RTK system (EGF/EGFR) may shape one canonical Gi/GPCR system (the chemokine system, CXCL12/CXCR4) via phosphorylation of Gαi. We find that the phosphoevents inhibit different aspects of signaling and do so through a variety of mechanisms, with the location of the phosphosites clusters on the G protein being a key determinant of how such inhibition is orchestrated.

RESULTS

Unique sites on Gαi are phosphorylated in the presence of epidermal growth factor (EGF)

To determine which residues on Gαi are phosphorylated in the presence of growth factors, we conducted in-cell kinase assays and analyzed the immunopurified Gαi3 by linear ion-trap mass spectrometry (MS) (31) (see *Methods* and **Figure 1a** for workflow). As for the choice of growth factor, we studied the EGF/EGFR system not only because EGFR is the prototypical growth factor RTK, but also because it is the most widely studied RTK for pathway crosstalk with GPCRs (32-34). Two independent MS analyses were performed; each time, samples were processed without any phosphoenrichment to allow for the assessment of the relative stoichiometry of the various phosphosites. Different sets of phosphorylated peptides were identified (**Figure 1b**); 7 sites were prioritized based on their confidence score, location within the G protein and corroboration in independent LC/MS studies (see **Table 1**). Projection of these residues on a topology map of Gαi3 (**Figure 1c**) and a solved crystal structure of the highly homologous Gαi1 (**Figure 1d**) revealed that phosphorylated positions are located in some of the key regions within Gαi, spanning both all-helical (AHD) and Ras-like domains, the nucleotide binding site, and the interdomain cleft. For example, S44, S47 and T48 are in the phosphate-coordinating P loop, S151 and Y154/Y155 are in the αE helix where they stabilize the αF helix and the conformational Switch-I (Sw-I), and Y320 is in the β6 strand where it interacts with the C-terminal α5 helix directly engaging with activated GPCRs (35). Barring two recently reported tyrosine (Y154/Y155) that are phosphorylated by RTKs within the interdomain cleft of Gαi (5), the other sites remain uncharacterized and their importance unknown.

Previously, the role of Gαi residues in the formation and stability of nucleotide-bound Gαi states or GPCR(rhodopsin)•Gαi complexes has been characterized at a single aa level by alanine (Ala; A) scanning mutagenesis (35). A re-analysis of the original dataset revealed that both P-loop residues S47 and T48 are critical for GTP binding, with T48 also being important for GDP binding, whereas mutations in S44 do not have much impact on either state (**Figure 1e**-*top*). Ala mutations of the interdomain cleft residues S151 and Y155 destabilized the GDP-bound state to a greater extent than the GTP-bound state; while elimination of Y154 did not have much impact on either state (**Figure 1e**-*top*). The C-terminally located Y320 was required for GPCR•Gαi complex formation and stability (**Figure 1e**-*bottom*); however, Ala substitution at this site had only a moderate effect on the nucleotide-bound states (**Figure 1e**-*top*) and no effect on heterotrimer formation (35). These findings suggest that phosphorylation at residues located in the P-loop and those buried within the interdomain cleft may primarily alter the kinetics of nucleotide exchange on the Gαi protein (and consequently its activity, conformation, and ability to sequester or release Gβγ), whereas phosphorylation at the C-terminal Y320 may primarily impair receptor engagement/recruitment.

Finally, the unique phosphosites identified in the presence of EGF were compared to phosphoevents on Gαi1-3 previously detected by high throughput mass spectrometry (HTP-MS) (21, 23, 24, 26, 36, 37) [cataloged at phosphosite.org], and with previously reported sites of somatic mutations in cancer [cataloged in the COSMIC database]. Such analysis showed that, in most instances, phosphoevents and mutations tend to cluster in the

same three regions of the Gαi protein: P-loop, interdomain cleft, and the C-terminus, implying that these could represent 'hot spots' within the allosteric switch.

Taken together, these findings suggest that the residues we selected to study further in this work (**Figure 1b; Table 1**) may have interesting and meaningful consequences for heterotrimeric G protein signaling.

Study design and rationale

To study the impact of phosphorylation on G protein signaling, we next generated phosphomimicking (S→D; T→E, Y→E), and in the case of Y320, non-phosphorylatable (Y→F) mutants of these residues (see **Table 2**). Our decision to make them as single mutations, or as combinations, was guided by their location, concomitantly phosphorylated state in cells (**Figure 1b**; **Table 1**), and by theme (i.e., pan-tyrosine or pan-Ser/Thr/Tyr). Because Ala substitutions at S/T sites strongly impact the stability and properties of Gαi (**Figure 1e**), their use as non-phosphorylatable S/T→A substitutions was deemed inappropriate and hence, not attempted. To enable functional characterization without the interference of endogenous G protein, all mutations were generated in a Gαi3 construct in which a cysteine (Cys; C) at position 351 was mutated to isoleucine (Ile; I): this C351I mutation renders the G protein insensitive to pertussis toxin (PTX) (38) and allows, in conjunction with PTX treatment, to selectively assess the GPCR-related functions of the mutant G protein (39). Consequently, in all our assays, the PTX-sensitive wild-type Gαi3 (WTs) and the PTX-resistant wild-type Gαi3 (WTr) served as negative and positive controls, respectively.

To assess the impact of the phosphomimicking Gαi mutations on canonical GiPCR signaling we used the prototypical GiPCR, the CXC chemokine receptor 4 (CXCR4), which couples to and transmits its signals through the PTX-sensitive G_i proteins (40). We chose CXCR4 because of the well-studied Gi-mediated signaling pathways that it activates in response to its endogenous chemokine agonist CXCL12, and because of its importance in cancer invasion and metastasis (40); the latter is a process that is enriched in pathway crosstalk between growth factors and GPCRs (32). In the case of CXCR4, prior studies have alluded to the presence of pathway crosstalk with the EGF/EGFR pathway and role of such crosstalk in promoting tumor progression (41).

As a model system for our studies of CXCR4-driven Gαi3 signaling, we chose HeLa cells because of their high level of endogenous CXCR4 (42) and responsiveness to CXCL12 (42).

Impact of the Gαi phosphomimicking mutations on canonical Gi-PCR-mediated Gβγ signaling

Next we assessed Gβγ release from the activated heterotrimeric Gαi/Gβγ complex, which is one of the earliest steps and a key event in the transduction of GiPCR signals (43, 44). We assessed Gβγ release and activation using agonist-induced changes in BRET (bioluminescence resonance energy transfer) between mVenus-tagged Gβγ (BRET acceptor) and RLuc8-tagged C-terminus of G protein-coupled receptor kinase-3 (GRK3ct) (BRET donor) (**Figure 2a-b**). A CXCL12-induced increase in BRET ratio indicates dissociation of the Gαi/Gβγ

heterotrimer and release of free Gβγ, which then becomes available for interaction with GRK3ct. A higher BRET ratio at baseline indicates excess free Gβγ dimers, likely due to the compromised ability of mutant Gαi to sequester Gβγ and form stable Gαi/Gβγ heterotrimers. After confirming that exogenous transfection of various Gαi mutant constructs in HeLa cells result in comparable expression (**Figure 2c-d**), BRET was assessed with or without PTX pretreatment and with or without CXCL12 stimulation (a total of four conditions) (**Supplementary Figure 1a-b**). The three variants containing phosphomimicking modifications of Y154 and Y155 (YY154-155EE, YY154-155EE, and pan-S/T/Y) demonstrated significant decreases in the basal suppression of BRET signal when compared to the positive control WTr, and no differences when compared to the negative control (pcDNA, no transfected Gαi) (**Figure 2e-f; Table 3**-*column #3*), indicating that these mutants are severely impaired in Gβγ binding. These mutants also failed to show an increase in BRET ratio (indicative of Gβγ release) upon ligand stimulation (**Figure 2g-h; Table 3**-*column #4*), consistent with their inability to bind Gβγ in the first place. By contrast, the P-loop mutants were either proficient (S44D) or partially proficient (S47D-T48E) in Gβγ sequestration at baseline (p values of 1.5e-4 and 4.1e-2 respectively, when compared to the negative control pcDNA; and p values of n.s and 4.4e-5, respectively, when compared to the positive control WTr); however, they were still defective in Gβγ release upon ligand stimulation (both not significantly different from negative control WTs; p value <1e-7 for both S44D and S47-T48E when compared to the positive control WTr). This may be a consequence of the inability of these mutants to bind GTP: Gβγ release requires that Gαi is GTP-bound, but for at least two other substitutions at position 47 of Gαi (Ala and Asn), severe impairment of GTP binding has been previously reported (35, 47), with S47N also preferentially stabilizing (or trapping) a nucleotide-free, GPCR-bound state of the Gαi/Gβγ heterotrimer (45-47) Additionally, an Ala substitution at position 48 has been shown to abrogate the binding of both GDP and GTP (43). As for the C-terminal phosphosite Y320, the phosphomimic Y320E substitution was partially deficient in Gβγ sequestration and incapable of Gβγ release after ligand stimulation. By contrast, the Y320F mutant was fully and partially proficient in Gβγ sequestration and release, respectively, suggesting that phosphorylation of Gαi at Y320 may be sufficient to inhibit canonical Gi signaling. Interestingly, although the double YY154-155EE mutant and the triple YYY154-155-320EEE mutant were both inert in basal Gβγ sequestration (**Figure 2f**) and ligand stimulated Gβγ release (**Figure 2h**), a replacement of Y320 by the non-phosphorylatable "F" led to a mutant (YYY154-155-320EEF) that regained full proficiency in both Gβγ sequestration (p value = 4e-7 compared to negative control, and not significantly different from positive control) and partial proficiency in ligand-stimulated Gβγ release (p value <1e-7 and 5.6e-5 compared to negative and positive controls, respectively). This indicates that the Y320F substitution rescued the defects observed in the double Y→E mutant within the interdomain cleft (*p* value <1e-7 for both basal sequestration and ligand-induced release; see **Table S1-S2; Table 3**-*column #3-4*).

These findings indicate that growth factor-triggered phosphomodifications in Gαi can modulate the canonical Gβγ signaling in at least three ways: (i) impair the ability of the Gαi to form trimers with Gβγ at basal state, and consequently, inhibit canonical ligand-induced signaling while allowing for constitutive activation of Gβγ (exemplified by phosphomimicking mutations at the interdomain cleft and at the C-terminus); (ii) inhibit

ligand-stimulated Gβγ release but preserve, partially or fully, the ability to sequester Gβγ and form trimers at basal state (such as S/T phosphorylation in the P-loop). Pan-phosphorylation at all S/T/Y sites follows the first pattern. Intriguingly, phosphorylation at Y320 (mimicked by E) was sufficient to inhibit signaling, regardless of whether it was assessed independently by comparing Y320E vs Y320F (*p* value 0.0014 for Gβγ sequestration and 7.0e-7 for Gβγ release, respectively; **Table S1-S2**) or in combination with other phosphotyrosines by comparing YYY154-155-320EEE vs YYY154-155-320EEF (*p* values <1 e-7 for both basal Gβγ sequestration and ligand-induced Gβγ release; **Table S1-S2; Table 2**-*column #3-4*). Even more interesting, the non-phosphorylatable Y320F appears to rescue defects caused by the double YY154-155EE mutation.

Impact of the Gαi phosphomimicking mutations on canonical Gi-PCR-triggered cyclic AMP inhibition

As a $G\alpha_i$-coupled chemokine receptor, CXCR4 inhibits adenylyl cyclase activity and decreases intracellular cAMP (48); we asked what, if any, impact the phosphomodifications have on this key step in chemokine signaling. To this end, we used the established BRET-based sensor for cAMP, CAMYEL (cAMP sensor using YFP-Epac-RLuc), which can monitor intracellular concentrations of cAMP in real time in live cells (49) (**Figure 3a**). By the design of the sensor, a decrease in BRET ratio (acceptor emission divided by donor emission) corresponds to an increase in cAMP; therefore, for an intuitive display, in **Supplementary Figure 2b**, we expressed results of this assay as inverse BRET (donor emission divided by acceptor emission); for **Supplementary Figure 2a** and **Figure 3**, this quantity was further converted into cAMP suppression. As before, BRET was assessed in cells pre-treated (or not) with PTX and stimulated (or not) with CXCL12 (**Figure 3b**). Cellular luminescence was initiated by the addition of 10 μM coelentrazine-H mixed with 100 μM of phosphodiesterase inhibitor IBMX (the latter to prevent rapid degradation of intracellular cAMP). BRET was read immediately after this, then after the addition of buffer or 100 nM CXCL12, and finally after the addition of the adenylate cyclase activator Forskolin (FSK) (**Figure 3b**). Basal suppression or CXCL12-induced suppression of FSK-induced cAMP were computed as % compared to negative control [the PTX-sensitive wild-type Gαi3 (WTs)] set at 0% and the positive control [PTX-resistant wild-type Gαi3 (WTr)] set at 100%. Compared to the positive control WTr, none of the mutants significantly impacted the basal suppression of FSK-induced cAMP (**Supplementary Figure 2a**). In chemokine-induced cAMP suppression, the P-loop (S47/T48), the β6-strand (Y320E), the pan-Y (YYY154-Y155EEE), and the pan-S/T/Y mutants were significantly different from the positive control and no different from the negative control (**Figure 3c-d**; **Supplementary Figure 2b**; **Table 2**-*column #5*), indicating that these mutations abrogated CXCL12-induced cAMP suppression by Gαi. This was similar to their impairment in ligand-induced Gβγ release. By contrast, S151D and YYY154-155-320EEF were no different from the positive control and significantly different from the negative control, indicating that they retained the cAMP suppression ability. The rest of the mutants (S44D, YY154-Y55EE, and Y320F were not significantly different from either positive or negative control so that no conclusions could be made about their impact on the cAMP suppression.

These findings indicate that growth factor-triggered phosphomodifications in Gαi can modulate the canonical Gαi cAMP signaling pathway in at least two ways: (i) impair the ability of the ligand to suppress cAMP (exemplified by phosphorylation at S47 and T48 in the P-loop or the tyrosine phosphorylation at the C-terminus); (ii) neutral, i.e., exerts no effect (exemplified by a selected phosphoserine-mimicking mutation in the interdomain cleft (S151). Intriguingly, the phosphomimicking mutation at Y320 (Y320E) is sufficient to inhibit signaling, whereas the combination of the non-phosphorylatable Y320F mutant with YY154-155EE does not appear to be significantly compromised (**Table 2**-*column #5*).

Phosphomimicking and non-phosphorylatable mutations at Y320 impact Gαi recruitment to the receptor

Because of the profound and distinct effects of phosphomimicking mutation Y320E and non-phosphorylatable mutation Y320F on the canonical signaling of Gαi, and because of the location of Y320 in the Gαi β6 strand where it directly contacts the GiPCR and the GiPCR-engaging C-terminal α5 helix of Gαi (35) (**Figure 4a**), we asked if/how the Y320E/F mutants impact coupling of Gαi to GPCR. To assess receptor recruitment, we used a well-defined BRET-based assay in which Venus-tagged engineered "mini" Gα proteins engage RLuc-tagged receptors (50). Mini Gα proteins lack membrane anchors, N-terminal Gβγ-binding surface, and the α-helical domain (AHD), and contain a nuclear export signal (NES) (50). Ligand-induced coupling of a miniGα to an RLucII-tagged GPCR results in higher BRET ratio (**Figure 4b**). For Gi coupled receptors, the appropriate miniGα is miniGαs/i, a chimera between Gαs and Gαi. We confirmed by sequence alignment that Y320 in Gαi is conserved in the Gαs, and that the engineered miniGαs/i protein also contains a Y at the corresponding position (**Figure 4c**); the corresponding Y in miniGαs/i was then mutated to either the phosphomimicking E or the non-phosphorylatable F. We used these mutants alongside the WT miniGαs/i in a BRET acceptor saturation experiment, in which the transfected amount of the donor (RLucII-tagged CXCR4) is kept constant while the amount of the acceptor (Venus-tagged miniGαs/i-WT or the Y320E/F mutants) is titrated. Variation in acceptor expression levels was quantified by flow cytometry (**Supplementary Figure 3**). The resulting baseline-corrected BRET ratio plotted against fluorescence showed that ligand stimulation resulted in GPCR coupling with the expected saturable profile in the case of miniGαs/i-WT (**Figure 4c**). While both Y320E and Y320F mutants showed significant impairment in coupling to the GPCR (**Figure 4c-d**), the Y320F mutant reached saturation in GPCR coupling at a lower concentration of the acceptor compared to the Y320E mutant (**Figure 4c**). Additionally, once formed, the complexes between RLuc-tagged CXCR4 and Venus-tagged WT miniGαs/i remained stable for a long time, whereas the mutant complexes rapidly dissociated (**Figure 4d**).

These findings demonstrate that Y320 is a key determinant of GPCR coupling; while both Y320E/F mutants are somewhat impaired compared to the WT G protein, Y320F saturates the available receptors at a lower transfected amount of the G protein (**Table 2**-*column #6*). We conclude that growth-factor triggered phosphorylation of Gαi at Y320 may be sufficient to uncouple the G protein from Gi-PCR, which is in keeping with prior observation that growth factor stimulation leads to the release of Gαi from CXCR4 (51).

Impact of the phosphosites on canonical Gi-PCR-stimulated chemotaxis

Next we asked if the overall theme of inhibition that we observe in the canonical Gαi-mediated cAMP and Gβγ signaling cascades is physiologically relevant, i.e., translates into phenotypic changes in cells. To answer this, we chose to study directional migration, i.e., chemotaxis, because the CXCL12/CXCR4 system is known for its ability to support chemotaxis via a Gαi-dependent signaling axis (52). We used a well-accepted 3D-transwell assay in which HeLa cells were allowed to migrate across a 0-40 nM CXCL12 gradient for 20 h in the presence of PTX (**Figure 5a**). The positive and negative controls in our assay behaved as expected, i.e., cells expressing the PTX-sensitive WTs (negative controls) did not migrate, whereas those expressing the PTX-resistant WTr (positive controls) migrated (**Figure 5b**-*top panels*; **Figure 5c**). When compared against the PTX-resistant WTr, all but one mutant showed various degrees of impairment in their ability to drive chemotaxis (**Figure 5b-d**); the YYY154-155-320EEF mutant performed just as well as WTr. The YYY154-155-320EEF mutant was significantly more competent in chemotaxis in head-to-head comparisons with the virtually immotile YYY154-155-320EEE and YY154-155EE mutants (*p* values 0.009 and 0.014, respectively; **Table S4**). These findings indicate that the Y320F substitution was sufficient to reverse the inhibitory effects observed in Y→E mutants within the interdomain cleft.

These findings indicate that growth factor-triggered phosphomodifications in Gαi generally inhibits the canonical Gi-PCR-driven chemotaxis process, as exemplified by almost all the mutants, i.e., S/T phosphorylation at S44, S47 and T48 in the P-loop and tyrosine phosphorylation at the interdomain cleft and at the C-terminus. Consistent with all other readouts, the phosphomimicking mutation at Y320 was sufficient to inhibit chemotaxis, alone or in combination with YY154-155EE (**Table 2**-*column #5*). Intriguingly, as in the Gβγ release and activation assay, making Y320 non-phosphorylatable (Y320F) rescued the deficiencies of not only the triple phosphomimic YYY154-155-320EEE but also the double mutant YY154-155EE.

Structural analysis of phosphomimicking and non-phosphorylatable Gαi mutations

To put these experimental findings in a structural context, we projected the mutated residues on the Gαi structure in three structurally characterized functional states: inactive GDP-bound with Gβγ, nucleotide-free in complex with a GPCR and Gβγ (this transient state corresponds to nucleotide release), and active GTP-bound (**Figure 6a**). This revealed the proximity and interaction of all three P-loop residues with the nucleotides, with T48 directly coordinating the first phosphate for both GDP and GTP, S47 the Mg2+ ion in the GTP-bound state, and S44 forming a hydrogen bonding network with K45 and the second GDP/GTP phosphate. These observations suggest that phosphorylation (or phosphomimicking mutations) at these positions would disrupt the ability of Gαi to bind nucleotides and hence participate in the GDP/GTP exchange cycle in response to GiPCR stimulation. In

the nucleotide-free GPCR-bound state, these residues do not form any critical contacts which is likely why their mutations may trap this state, similar to (46).

The S151/Y154/Y155 residue cluster in the aE helix is engaged in a dense hydrogen-bonding network in both nucleotide-binding states, which is partially released in the domain-open, nucleotide-free state (**Figure 6a**). In fact, Y155 is fully buried in all structurally characterized states of Gαi, suggesting that for it to be phosphorylated the AHD must partially unfold. Y154, however, may become exposed through a rotamer change, especially in the nucleotide-free state.

The most interesting structural observations are related to Y320 in the β6 strand. In the nucleotide-bound states, this residue packs against the receptor-engaging C-terminal α5 helix and hydrogen-bonds to N346 (**Figure 6a**). In the process of Gαi activation by the receptor, due to a rotation and an upward shift of the α5 helix, this residue switches its hydrogen bonding to K345 and D341, while continuing to provide the stabilizing/packing interactions for that helix. In other words, Y320 works both as a stabilizing residue and a conformational switch in the process of Gαi activation by a GPCR. We hypothesize that Y320 phosphorylation or its replacement by E impairs the stability of the C-terminal α5 helix and may, for example, make it more prone for leaving its location in the center of the Gαi GTPase domain β-barrel (53, 54). By contrast, a Y320F substitution still allows this residue to serve its stabilizing role for the a5 helix, as only the hydrogen bond switching functionality is eliminated by that mutation.

Next, we computationally assessed the stability of the various structurally characterized functional states of Gαi when mutated at the phosphorylated positions. Four states functional states were assessed: nucleotide-free in complex with a GPCR and Gβγ, GDP-bound, GTP-bound with Gβγ, and GTP-bound), and multiple experimental structures were included where available. The effects of mutations on stability of each state was calculated and expressed as predicted ΔΔG of folding, with positive numbers indicating destabilization (state disfavored) and negative numbers indicating stabilization (state favored) (**Figure 6b** and **Supplementary Figure 4**).

S44D and S151D were predicted to slightly favor the nucleotide-free receptor- and Gβγ-bound state. In keeping with prior experiments (35, 46) S47D strongly disfavors the GTP-bound state of Gαi and T48D the GDP-bound state. Phosphomimicking mutations at Y154 and Y155 were predicted to be strongly destabilizing across the board, with a somewhat milder impact on nucleotide-free receptor- and Gβγ-bound Gαi. Similarly, Y320E was strongly destabilizing, with the GDP/Gβγ-bound state of Gαi affected the most (**Supplementary Figure 4**). By contrast, Y320F had only a minor destabilizing effect, and the GDP-bound states were affected the least (**Figure 6b** and **Supplementary Figure 4**).

In summary, these structural and computational observations provide a rational basis for the experimentally observed effects of the mutations.

Impact of the phosphomimicking and non-phosphorylatable mutations on membrane localization of Gαi

The contrasting effects of the phosphomimicking Y320E (and YYY154-155-320EEE) and the non-phosphorylatable Y320F (and YYY154-155-320EEF) substitutions across all readouts (**Table 2**-*columns #3-7*) led us to hypothesize that the non-phosphorylatable Y320F substitution may provide an advantage that drives the observed proficiency of the G protein in most assays. Because all mutants expressed at similar levels in cells (**Figure 2c-d**), difference in protein stability was deemed as an unlikely factor, and instead, we investigated protein localization. Confocal immunofluorescence studies carried out in HeLa cells revealed striking difference in the localization pattern between the E and F mutants (**Figure 6a**) Gαi proteins in which a Tyr/Y or a Phe/F occupy the position 320 (Y320F, YY154-155EE and YYY154-155-320EEF) localize predominantly at the peripheral membrane, presumably the plasma membrane (PM); however, proteins with a Glu/E at that position (Y320E and YYY154-155-320EEE) localize predominantly in the cytosol. Furthermore, cell fractionation assays confirmed these findings; ~55-65% of the mutant proteins with Y/F at position 320 was detected in the crude membrane fractions, as opposed to ~37-47% of the mutant proteins with E at position 320; the latter showed a shift from crude membrane to the cytosolic fraction (**Figure 6b**).

These findings demonstrate that Y320 on Gαi is a key determinant of G protein localization. That the Y320E mutant localizes to the cytosol but Y320F localizes at the PM, indicates that phosphorylation at Y320 may be sufficient for Gαi mislocalization. That the YY154-155EE and YYY154-155-320EEF mutants localize at the PM but YYY154-155-320EEE localizes to the cytosol indicates that phosphorylation at Y320 may be required for Gαi to lose PM localization (**Table 2**-*column #8*).

DISCUSSION

The canonical trimeric G protein signaling is triggered by ligand activated GPCRs; however, the canonical GPCR pathways have been shown in many contexts to be subject to crosstalk and regulation by growth factors. Here we reveal the molecular mechanisms that enable growth factor RTKs to modulate the canonical G protein signaling. More specifically, we show that growth factors shape canonical signaling, at least in part, through phosphorylation of Gαi (**Figure 7c**). Phosphorylation occurs at key residues (clusters of residues) located at three strategic hot spots within the GTPase: the P-loop, the interdomain cleft and the C-terminus. Using a library of phosphomimicking mutants in a series of assays to interrogate some of the most upstream (receptor recruitment and trimer dissociation) as well as downstream (cAMP inhibition and chemotaxis) events in canonical Gi/GPCR signaling, we show that the phosphomodifications predominantly inhibit ligand-induced signaling with some of them also promoting constitutive Gβγ signaling. These findings illuminate the basis for some poorly-understood observations by others that growth factors (EGF and IGF1) inhibit Gi coupling to and activation by GPCRs (CXCR4) (30, 51). We also show that the mechanism(s) for signal inhibition differs based on the location of the phosphosites within the G protein (see **Figure 7c; Table 3**-*columns #9-10*). These findings are discussed below.

First, phosphorylation of key residues at the interdomain cleft, i.e., S151, Y154 and Y155 (which are phosphorylated in combinations of pS151 alone and pY154/pY155) we find that while S151 has little or no impact, the pair of Ys impair ligand stimulated Gβγ release, partially impair ligand stimulated cAMP suppression, and inhibit chemotaxis. Importantly, all of this occurs in the background of elevated constitutive Gβγ signaling due to the impairment of the mutated/phosphorylated Gαi ability to bind and sequester/inactivate Gβγ. Computational analyses revealed that phosphorylation at Y154/Y155 may favor the nucleotide-free conformation. These findings are consistent with our prior work (using non-phosphorylatable mutants in FRET-based assays) which showed that dual phosphorylation at Y154/Y155 is required for growth factor stimulated trimer dissociation and increases basal nucleotide exchange rate (~5-fold higher than WT) (5). Increased basal activity effect was attributed to disrupted intermolecular interactions and packing (loss of H-bonds) within the inter-domain cleft, which may affect opening/closing of the protein's all-helical and Ras-like domains (5). Although molecular dynamic simulation studies have shown that domain opening is insufficient for GDP release (55), phosphorylation at Y154/155 may affect neighboring residues within the nucleotide-binding pocket, such as those in the αD-αE loop which includes the so-called 'NDS^{151}' motif. Alternatively, because both Y154 and Y155 face towards αF and Sw-I, particularly Y155, it is possible that destabilization of Sw-I could serve as a mechanism for pTyr-induced allosteric activation of the GTPase; Sw-I was recently identified as a key conduit in the allosteric path to nucleotide release that is triggered by the guanine-nucleotide exchange factor, GIV/Girdin, transmitting forces from the Sw-II to the hydrophobic core of the GTPase (56). While the identity of the kinase that phosphorylates S151 remains unknown, Y154/Y155 has been shown to be phosphorylated by multiple RTKs (but not non-RTKs) (5). Regardless of who phosphorylates them and how these phosphosites impact the basal exchange rate, what is clear is that they functionally uncouple the G protein from GPCRs, by reducing Gβγ-binding and trimer assembly. In doing so, the interdomain cleft events segregate the RTK→Gαi pathway (with resultant higher basal activity) from the canonical GPCR→Gαi pathway.

Second, phosphorylation of key residues within the P-loop, i.e., S44, S47 and T48 (the latter two are simultaneously phosphorylated) impairs ligand-stimulated Gβγ release, and cAMP suppression, but largely spares the ability of the G protein to bind Gβγ and assemble trimers. Computational analyses revealed that phosphorylation at S47 preferentially destabilizes the GTP-bound state, whereas phosphorylation at T48 destabilizes the GDP-Gβγ-bound Gαi. These are not unexpected, because the P-loop, which is essentially the sequence ^{40}GAGESGKST^{48} (57), is known to participate in nucleotide binding and coordination of Mg^{2+} (58); while S47 coordinates the Mg^{2+}, T48 bridges the β and γ phosphates in GTP. Our findings are consistent with prior work in which phosphorylation at S44 on Gαi2 was implicated as a basis for desensitization of μ-opioid receptors (59). Similarly, the S47R mutant Gαi3 (implicated in auriculo-condylar syndrome (ACS)) produces dominant-negative proteins that couple to the GPCR but cannot bind and hydrolyze GTP (60). A similar effect has been observed in the case of Gαq (S53, which corresponds to S47 in Gαi); phosphorylation of this site impedes GTP-binding and downstream signaling events (61). Although the identity of the kinase(s) that phosphorylate these P-loop sites remains unknown, the phosphorylation functionally uncouples the G protein

from GPCRs, by reducing ligand-induced Gβγ-release but without elevating the constitutive Gβγ activity. Because coupling to Gβγ and GPCR is unlikely to be impacted, Gαi proteins phosphorylated at these sites may behave as dominant negative proteins that couple to the GPCR but cannot release Gβγ; nor will they bind and hydrolyze GTP. Thus, the P-loop sites may not only inhibit the canonical GPCR→Gαi pathway but carry the potential to exert a dominant negative effect.

Third, phosphorylation of Y320, a key residue at the C-term β6 strand, impairs Gβγ-binding and ligand-stimulated Gβγ release, receptor coupling, ligand stimulated cAMP suppression, and inhibits chemotaxis. A prior study had established the importance of this residue in coupling to GPCRs (35), and we previously established that Y320 is phosphorylated by RTKs, both *in vitro* and in cells (5). We found that phosphomimicking mutants of Y320, either alone or in combination with other tyrosines in the interdomain cleft, renders the G protein inert to canonical signals. Interestingly, a Y320F substitution not just retains Gβγ-binding, but also ligand-stimulated Gβγ release. To our surprise, Y320F could reverse defects in signaling observed in the proteins in which the two Y in the interdomain cleft region are phosphorylated. We found that one potential mechanism for these contrasting features is protein localization—proteins with Y320E (alone or in combination with mutants of the interdomain cleft) were cytosolic, whereas proteins with Y320/Y320F (alone or in combination) were localized to the PM. As for the mechanism by which Y320 dictates membrane localization, it is unlikely that the mechanism is either of the two known determinants of membrane localization of Gαi subunits, i.e., N-terminal myristoylation and/or palmitoylation and association with Gβγ dimers (17) (YY154-155EE, which is deficient in Gβγ-binding, is localized at the PM). What was also puzzling is that Y320E alone was sufficient to abrogate Gβγ-binding. Recently revealed structural insights (54) into how the G protein chaperone and guanine nucleotide exchange factor Ric-8 binds Gαi sheds some light on this puzzle. The core of the Gαi•Ric8 complex requires the β4-β6 strands of Gαi and Y320(β6) serves as a contact site (54), which raises the possibility that it may be a critical determinant of the interaction. It is noteworthy that the Y320E containing Gαi mutants in our system mimic the defects previously reported in Ric8-depleted diverse systems (fungi, fly, worm, and mammalian), i.e., Gαi subunits show reduced steady-state abundance at the PM, associate inefficiently with Gβγ dimers and consequently, assemble heterotrimers poorly (53, 62-66). Whether phosphorylation of Gαi at Y320 impacts its interaction with and modulation by Ric8 remains to be explored. Regardless, what emerged from this work is that phosphorylation at Y320 by growth factor RTKs impairs GPCR coupling and PM localization (cytosolic compartmentalization) of the Gαi protein and thereby, inhibits the canonical GPCR→Gαi pathway.

In conclusion, we show how diverse phosphoevents triggered by growth factors on Gαi exert a coherent effect, i.e., they all inhibit canonical GPCR signaling via distinct mechanisms that are dictated by the location of the phosphosites. Findings provide mechanistic into how growth factors inhibit canonical Gi/GPCR signaling insights from the level of the atoms to the level of the whole cell.

ACKNOWLEDGMENT: The authors thank Paul Insel and Tracy M. Handel (UC San Diego, CA, USA), Nevin A. Lambert (Augusta University, GA, USA) and Michel Bouvier (Université de Montréal, Canada) for their generosity in sharing receptor and reporter constructs.

FUNDING: This paper was supported by the NIH (CA238042, AI141630, CA100768 and CA160911 to P.G., R21 AI149369, R01 GM136202, R21 AI156662, and R01 AI161880 to I.K.).

AUTHOR CONTRIBUTIONS: S.R, I.K and P.G conceptualized the project; S.R, carried out all the experiments; I.K carried out all the computational analyses; M.G and P.G carried out the in cellular phosphorylation and LC/MS studies. S.R, I.K and P.G prepared figures for data visualization. S.R, I.K and P.G wrote the original draft of the manuscript. All authors provided input and edited and revised the manuscript. All co-authors approved the final version of the manuscript. I.K and P.G coordinated and supervised all parts of the project and administered the project.

COMPETING INTERESTS: The authors declare no competing interests.

DATA AND MATERIALS AVAILABILITY: All data for this research are included in the manuscript and in Supplementary Materials.

TABLES AND LEGENDS

Table 1. Phosphosites identified by linear ion-trap mass spectrometry. Red font indicates the sites studied in this work. * Sites reported as phosphorylated in phosphosite.org; † Sites neighboring nucleotide-binding pocket; £ Sites facing GPCR-binding interface.

Peptide sequence	Phospho form
AAVERS[Pho]K	pS16
DGGVQAC[Cam]FS[Pho]R	pS141
SREYQLNDS[Pho]AAY[Pho]YLNDLDR	pS151†
EYQLNDS[Pho]AAY[Pho]YLNDLDR	
RLWRDGGVQACFSRSREYQLNDS[Pho]ASY[Pho]YLNDLDR	
EYQLNDSASY[Pho]Y[Pho]LNDLDR	pY154/155
IS[Pho]QTNYIPTQQDVLR	pS163*
LLLGAGES[Pho]GK	pS44*†
S[Pho]T[Pho]IVKQK	pS47†/pT48†
TTGIVET[Pho]HFTFKELYFK	pT187
TTGIVETHFT[Pho]FK	pT190
S[Pho]KMIDR	pS16
VVVYSNTIQS[Pho]IIAIIR	pS263
EVY[Pho]THFTC[Cam]ATDTK	pY320*£

Table 2. Inventory of constructs and the annotation used in this work.

Constructs	Annotation	Comments
Gαi3	WTs	PTX sensitive
Gαi3 (C351I)	WTr	PTX resistant (working as backbone control for all the mutants)
Gαi3-S44D(C351I)	S44D	
Gαi3-S151D(C351I)	S151D	
Gαi3-Y320E(C351I)	Y320E	
Gαi3-Y320F(C351I)	Y320F	
Gαi3-S47D-T48E(C351I)	S47D-T48E	
Gαi3-YY154-155EE(C351I)	YY154-155EE	
Gαi3-YYY154-155-320-EEE(C351I)	YYY154-155-320EEE	
Gαi3-YYY154-155-320-EEF(C351I)	YYY154-155-320EEF	
Gαi3-S44D-S47D-T48E-Y154E-Y155E(C351I)	Pan-pS/T/Y	

Table 3. Summary of experimentally derived findings.

Construct	Name used	Basal Gbβγ association (or "sequestering")	Chemokine-induced Gβγ release and activation	Chemokine-induced cAMP suppression	Chemokine-induced receptor recruitment	Chemokine-induced chemotaxis	Protein localization	Location of phosphosite mutant	Impact on canonical Gi/GPCR signaling (MoA)
Gαi3 (-ve control, not resistant to PTX)	**WTs**	Proficient	Deficient in the presence of PTX	Deficient in the presence of PTX	NA	Deficient in the presence of PTX	NA	NA	Inert, as expected in the presence of PTX (Neg control)
Gαi3 C35I1 (+ control as it is PTX resistant)	**WTr**	Proficient	Proficient in the presence of PTX	Proficient	NA	Proficient	membrane	NA	Signals, as expected (Pos control)
S44D Gαi3 (C351I)	**S44D**	Proficient	**Deficient**	Inconclusive	NA	NA	NA	P-loop	Suppressed/Inhibited (stabilization of GDP and Gβγ-bound state)
S47D, T48E Gαi3 (C351I)	**S47D-T48E**	Partially proficient	**Deficient**	**Deficient**	NA	NA	NA		
S151D Gαi3 (C351I)	**S151D**	Proficient	Proficient	Proficient	NA	NA	NA	'NDS' seq; αF helix and Sw-I loop buried in the interdomain cleft	No impact
Y154E, Y155E Gαi3 (C351I)	**YY154-155EE**	**Deficient**	**Deficient**	Inconclusive	NA	**Deficient**	membrane		Suppressed (impaired trimer formation); increased basal activity (5)
Y320E Gαi3 (C351I)	**Y320E**	Partially proficient	**Deficient**	**Deficient**	Deficient	NA	cytosol	β6 sheet (C-terminus)	Suppressed (mislocalization and impaired GPCR binding)
Y320F Gαi3 (C351I)	**Y320F**	Proficient	Partially proficient	Inconclusive	Partially proficient	NA	membrane		(Rescued localization)
Y154E, Y155E, Y320E Gαi3 (C351I)	**YYY154-155-320EEE**	**Deficient**	**Deficient**	**Deficient**	NA	**Deficient**	cytosol	Combination	Suppressed (mislocalization)
Y154E, Y155E, Y320F Gαi3 (C351I)	**YYY154-155-320EEF**	Proficient	Partially proficient	Proficient	NA	Proficient	membrane		(Rescued localization)
S44D, S47D, T48E, Y154E, Y155E Gαi3 (C351I)	**Pan-pS/T/Y**	**Deficient**	**Deficient**	**Deficient**	NA	NA	NA		Suppressed (Inert in multiple readouts)

Glossary of terminologies [and their defining criterion] used to summarize the impact of mutation on G protein function:

- Deficient [non-significant compared to negative control and p-value<0.05 compared to positive control]
- Proficient [non-significant compared to positive control and p-value<0.05 compared to positive control]
- Partially proficient [when p value is <0.05 when compared to *both* positive and negative controls]
- Inconclusive [non-significant compared to either positive or negative control]

NA, not applicable or not assessed

n.s, not significant;

Neg, negative;

Pos, positive;

MoA, mechanism of action.

FIGURES AND LEGENDS

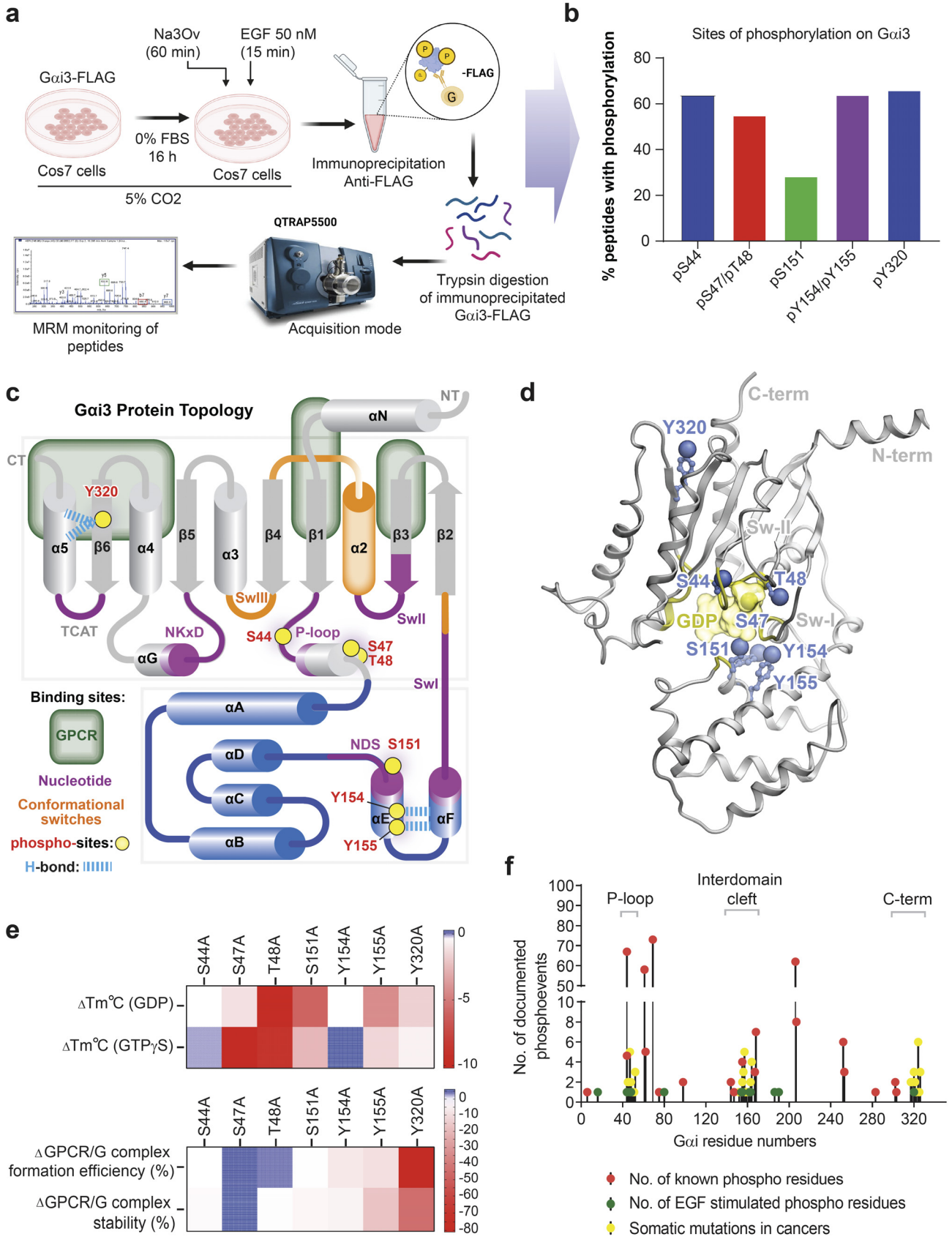

Figure 1. Phosphorylation analysis of Gαi3 in EGF-stimulated cells.

a. Schematic of the experimental workflow used to discover phosphosites on Gαi triggered in response to EGF. Briefly, serum-starved Cos7 cells co-expressing untagged EGFR and C-terminally FLAG-tagged Gαi3 were stimulated with 50 nM EGF. Gαi3 immunoprecipitated from cell lysates with anti-FLAG mAb was digested on Protein-G beads and the tryptic fragments were analyzed using LC/MS without any further phosphoenrichment steps (see *Methods* for details).

b. Bar graph displays the % phosphorylation of residues on Gαi3 (calculated as [phosphorylated peptides ÷ total detected peptides] x 100).

c-d. Phosphosites on Gαi3 that were identified by LC/MS in a-b are projected on a topology map of the Gαi3 protein (modified from (56)) with conformational switches and binding sites of key interactors marked (**c**) and on a ribbon diagram of the solved crystal structure of Gαi (PDB: 5tdh; **d**). Residues indicated in red highlight phosphosites which were mutated to phosphomimic (or non-phoshorylatable) aa in this work.

e. Heatmaps display the experimentally determined changes in the thermal stability of Gαi1 and its ability to form GPCR complexes upon mutating key phosphosites (identified in a-b) on into Ala(A) reported by a prior work (35). The thermal stability of each mutant is displayed (from top to bottom) in the inactive GDP-bound, the active GTP(GTPγS)-bound states, and the efficiency of formation (relative abundance) and relative stability of the reconstituted Rhodopsin-G_i protein complex. See also **Supplemental Information 3**.

f. Lollipop diagram shows all documented S/T/Y phosphorylation events on Gαi1, Gαi2, and Gαi3 and somatic mutations in cancers (red: data from Phosphosite.org; Green: Our experimental data; Yellow: Data from COSMIC; https://cancer.sanger.ac.uk/cosmic).

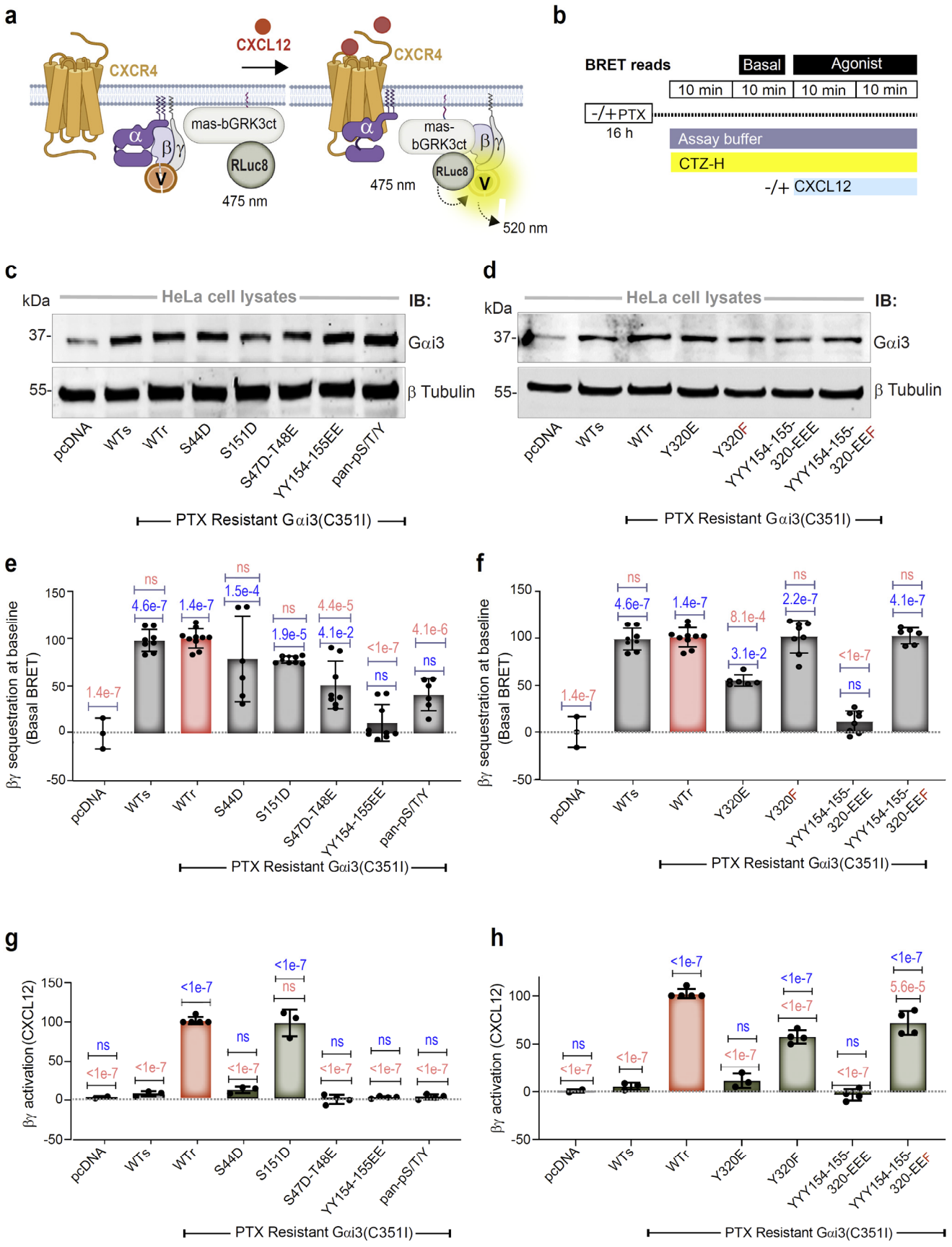

Figure 2. Effect of phosphomimicking mutations in Gαi3 on basal and CXCL12- stimulated Gβγ activation downstream of CXCR4.

a-b. Schematics of the principles (a) and the timeline for various treatments and readouts (b) of the BRET-based assay for assessing basal and ligand-stimulated Gβγ release from trimeric Gi. Prior to ligand stimulation (basal), Venus-tagged Gβ1/Gγ2 complexes bind Gαi●GDP to form inactive trimers. Upon addition of CXCL12, nucleotide exchange triggers the release of Venus-Gβγ dimers from Gαi which allows them to bind GRK3ct-RLuc8 and results in an increase of the BRET signal.

c-d. Immunoblots show the levels of expression of each phosphomimicking (or non-phosphorylatable) Gαi mutant in equal aliquots of lysates of HeLa cells (loading control, β-Tubulin).

e-f. Bar graphs display the % Gβγ activation observed in the case of each mutant at baseline. Results are expressed as fold change compared to the observed basal activity in the absence of transfected Gαi (pcDNA, set at 0%) and in the presence of PTX-resistant Gαi3 (WTr, set at 100%) in the PTX-treated condition.

g-h. Bar graphs display the % Gβγ activation upon ligand stimulation observed in the case of each mutant in **Table 1**. Results are expressed as fold change compared to the observed activity in the PTX-sensitive (WTs, set at 0%) and PTX-resistant (WTr, set at 100%) Gαi3 in the PTX-treated condition.

Statistics: *P* values were determined by one-way ANOVA with Tukey's multiple comparison's test. Values in blue and red fonts indicate significance compared to negative and positive controls, respectively. Error bars represent ± S.E.M; n=4 independent experiments, each with 3 technical replicates. In panels (e-f), PTX-treated and non-PTX treated samples from the same day were used as separate biological replicates thus producing n=8, each with 3 technical replicates. See also **Supplementary Figure 1** for the composite data for all conditions.

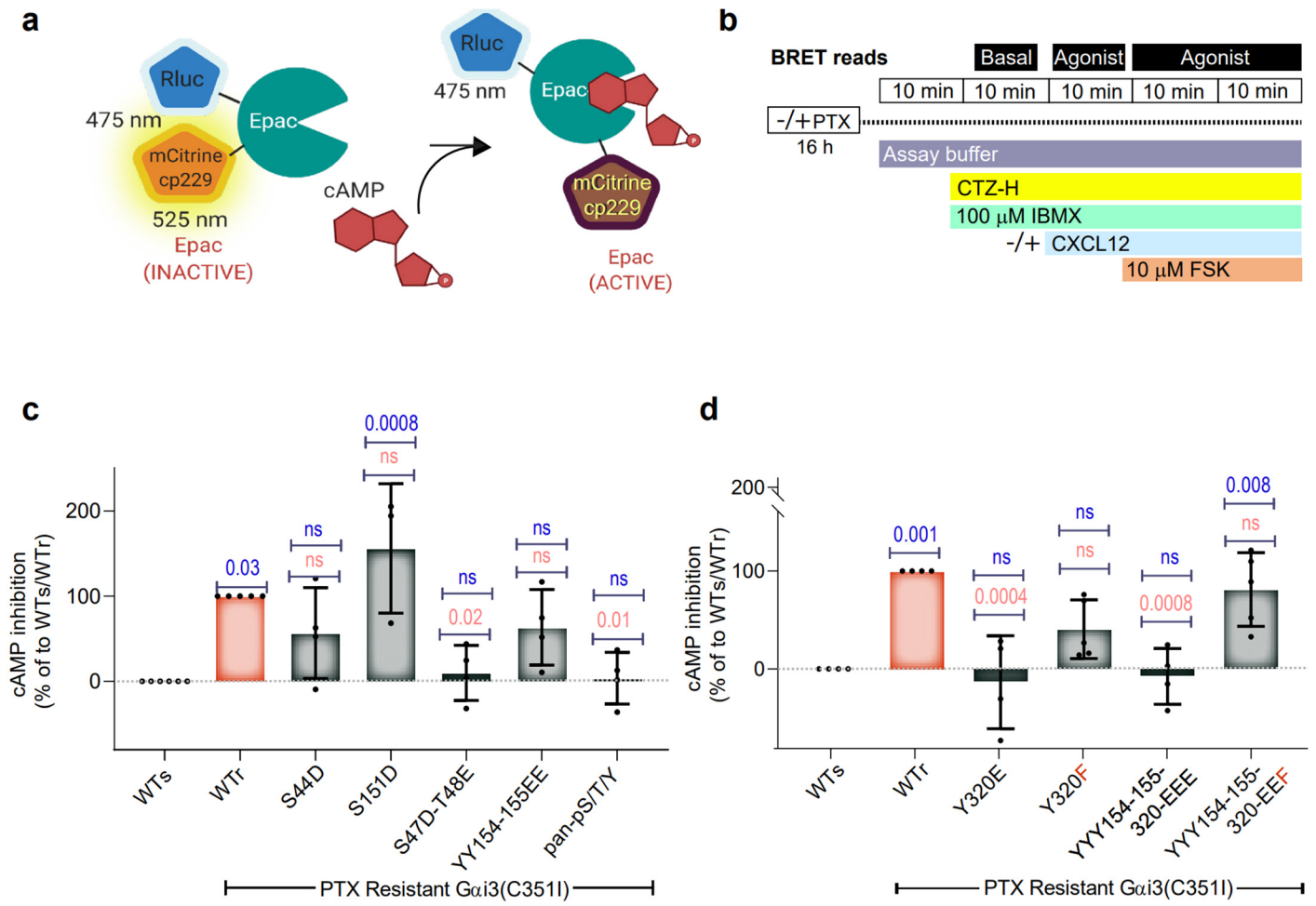

Figure 3. Effect of phosphomimicking mutations in Gαi3 on CXCL12-stimulated cAMP suppression downstream of CXCR4.

a-b. Schematics of the principle (a) and the timeline for various treatments and readouts (b) for the BRET-based CAMYEL (*cAM*P sensor using *Y*FP-*E*pac-R*L*uc) assay for assessing cAMP suppression by WT and mutant Gαi. Forskolin (FSK) is used to increase cellular cAMP, which, upon binding to CAMYEL, decreases the BRET signal. Activation of Gαi suppresses the extent of FSK-stimulated cAMP production, and consequently, increases the BRET signal.

c, d. Bar graphs display the % inhibition of cAMP upon ligand stimulation in the case of each mutant. Results are expressed as fold change compared to the observed inhibition in the sensitive (WTs, set at 0%) and PTX-resistant (WTr, set at 100%) Gαi3 in the PTX-treated condition.

Statistics: *P* values were determined by one-way ANOVA with Tukey's multiple comparison's test. Values in blue and red fonts indicate significance compared to the wild-type sensitive (WTs) and resistant (WTr) G protein, respectively. Error bars represent ± S.E.M; n=4 independent biological replicates, each with 3 technical replicates.

See **Supplementary Figure 2a** for the impact of each Gαi3 mutant on the basal FSK-stimulated cellular cAMP levels and **Supplementary Figure 2b** for each biological replicate.

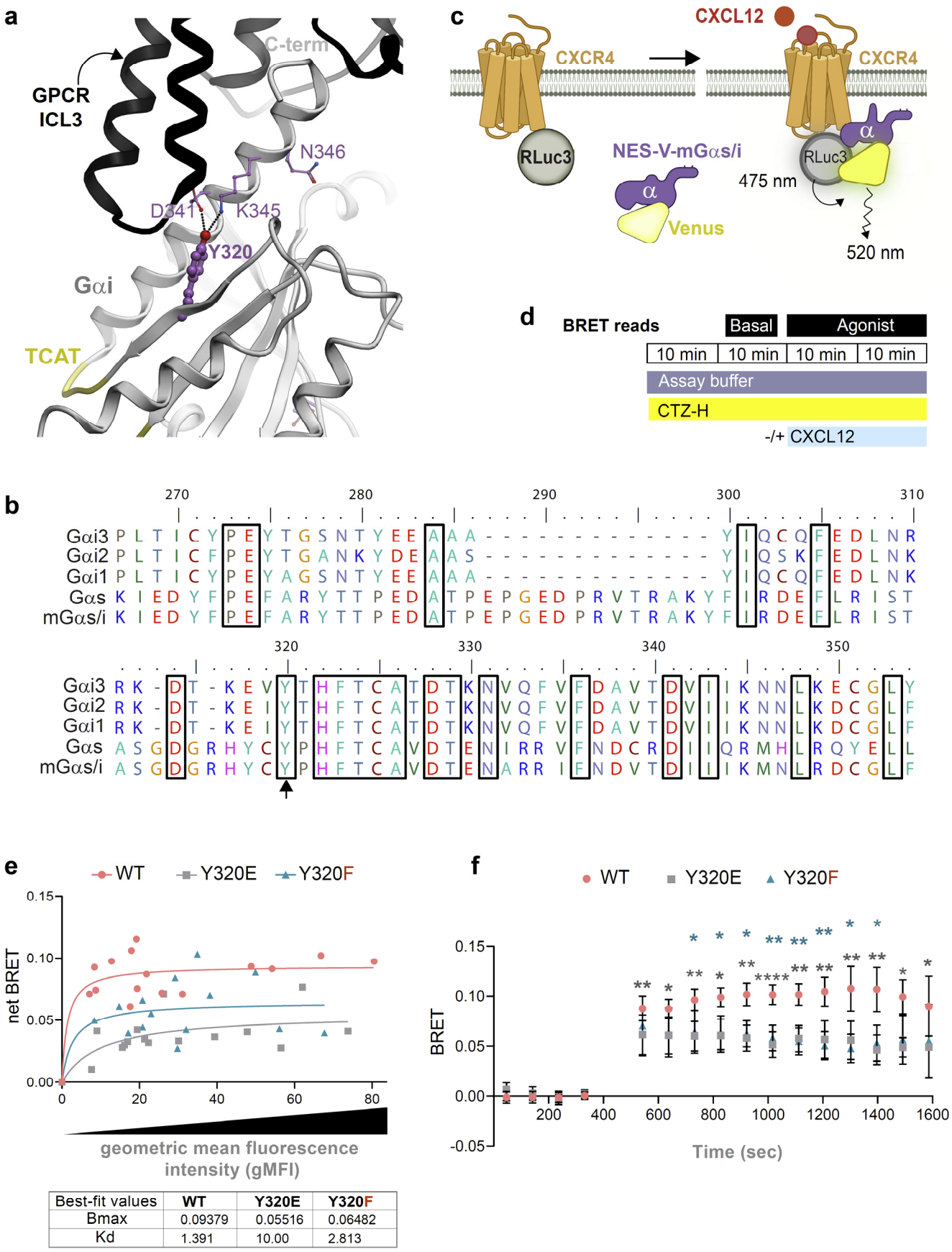

Best-fit values	WT	Y320E	Y320F
Bmax	0.09379	0.05516	0.06482
Kd	1.391	10.00	2.813

Figure 4: **Impact of phosphomimicking and non-phosphorylatable mutants of Y320 on GiPCR recruitment to Gαi.**

a. A ribbon diagram of the solved crystal structure of Gαi-bound GPCR (PDB: 6cmo) highlights the interaction surface of the GiPCR intracellular loop 3 (ICL3) with the C terminal α5 helix of Gαi. Crucial for the stabilization of the receptor-bound state are interactions between the β6 (Y320) and the α5 (D341, K345 and N346).

b. An alignment of rat Gαi1-3 sequences with Gαs and the mini-Gαs/i chimera used here is shown. Arrow highlights Y320.

c-d. Schematics of the principle (c) and the timeline for various treatments and readouts (d) of the BRET-based assay for assessing GPCR recruitment to the WT and mutant mini- Gαs/i chimeras. Proximity between the receptor (tagged with the BRET donor, Renilla luciferase 3) and the mini-Gαs/i (tagged with the BRET acceptor, Venus) results in energy transfer (see *Methods*).

e. Results of BRET saturation assays, where a fixed amount of donor (100 ng GPCR) is co-expressed with increasing amounts of the acceptor (0 ng to 2500 ng of mini-Gαs/i chimera DNA per well in a 6-well plate) are displayed as saturation plots of geometric mean fluorescence intensity (GMFI) on the x-axis against net BRET ratios on the y-axis. Shown are pooled results from 4 independent biological experiments, each with BRET measured in three technical replicates and GMFI measured in one replicate. A representative flow cytometry quantification for acceptor expression is shown in **Supplementary Figure 3**.

f. Time course graph shows baseline-corrected BRET before and after the addition of CXCL12 at a saturating transfected amount (2500 ng per well in a 6-well plate) of the acceptor DNA. The use of *, **, ***, **** mark significance levels, e.g., $p<.05$, $p<.01$, $p<.001$ and $p<.0001$). Colors (of *) reflect each mutant compared to WT.

Statistics: *p* values were determined by one-way ANOVA. Error bars represent ± S.E.M; n=4 independent biological replicates, each with 3 technical replicates.

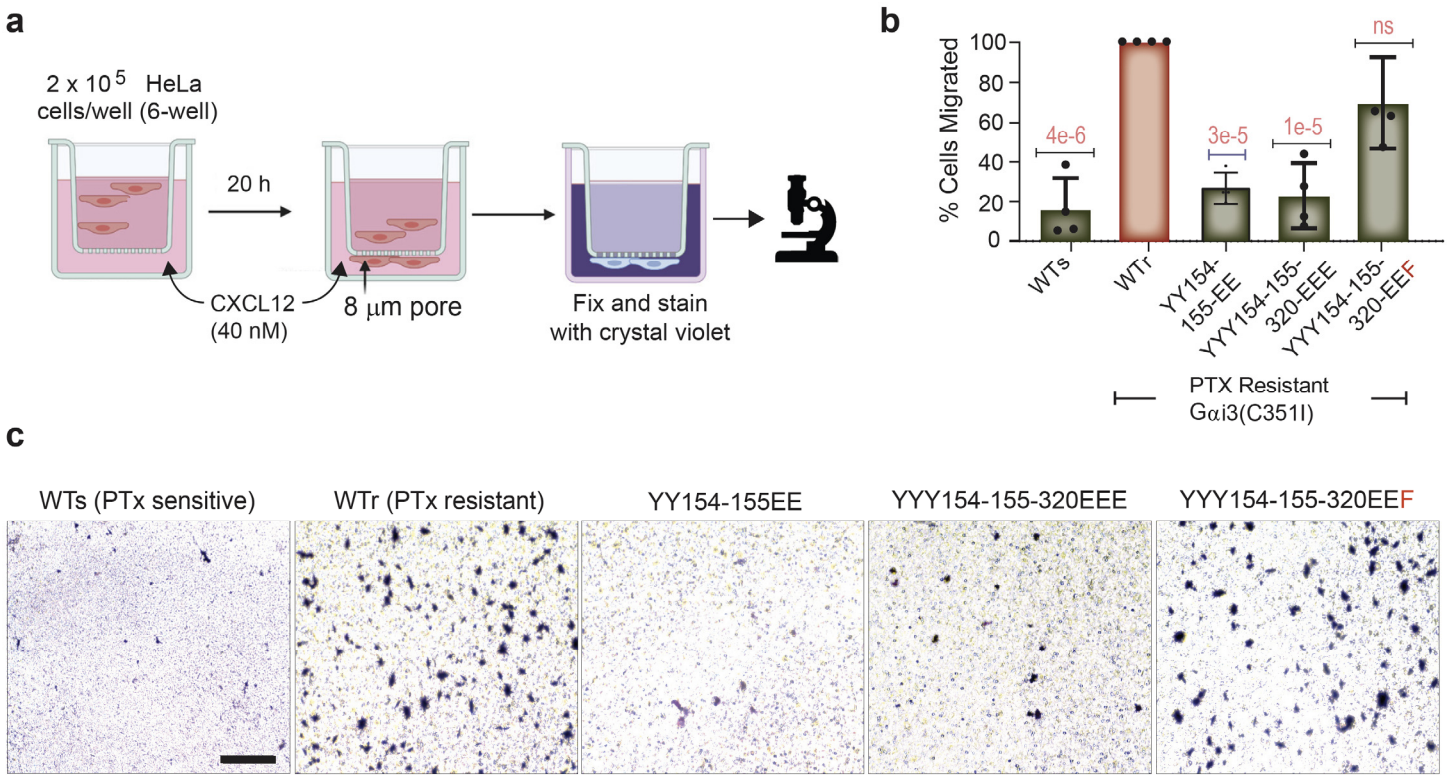

Figure 5: **A non-phosphorylatable mutant of Y320 rescues CXCL12- stimulated chemotaxis.**

a. Schematic displays the pertinent details of a transwell cell migration assay to measure the chemotactic capability of HeLa cells transiently expressing various Gαi3 mutants across a 0-40 nM CXCL12 gradient.

b. Bar graph shows % cell migration compared to cells expressing the wild-type PTX-resistant (WTr) Gαi3.

c. Representative images of crystal violet-stained transwell membrane are shown. Scale bar: 100 µm.

Statistics: *P* values were determined by one-way ANOVA followed by Tukey's multiple comparison test. Error bars represent ± S.E.M; n=4 independent biological replicates, each with 3 technical replicates.

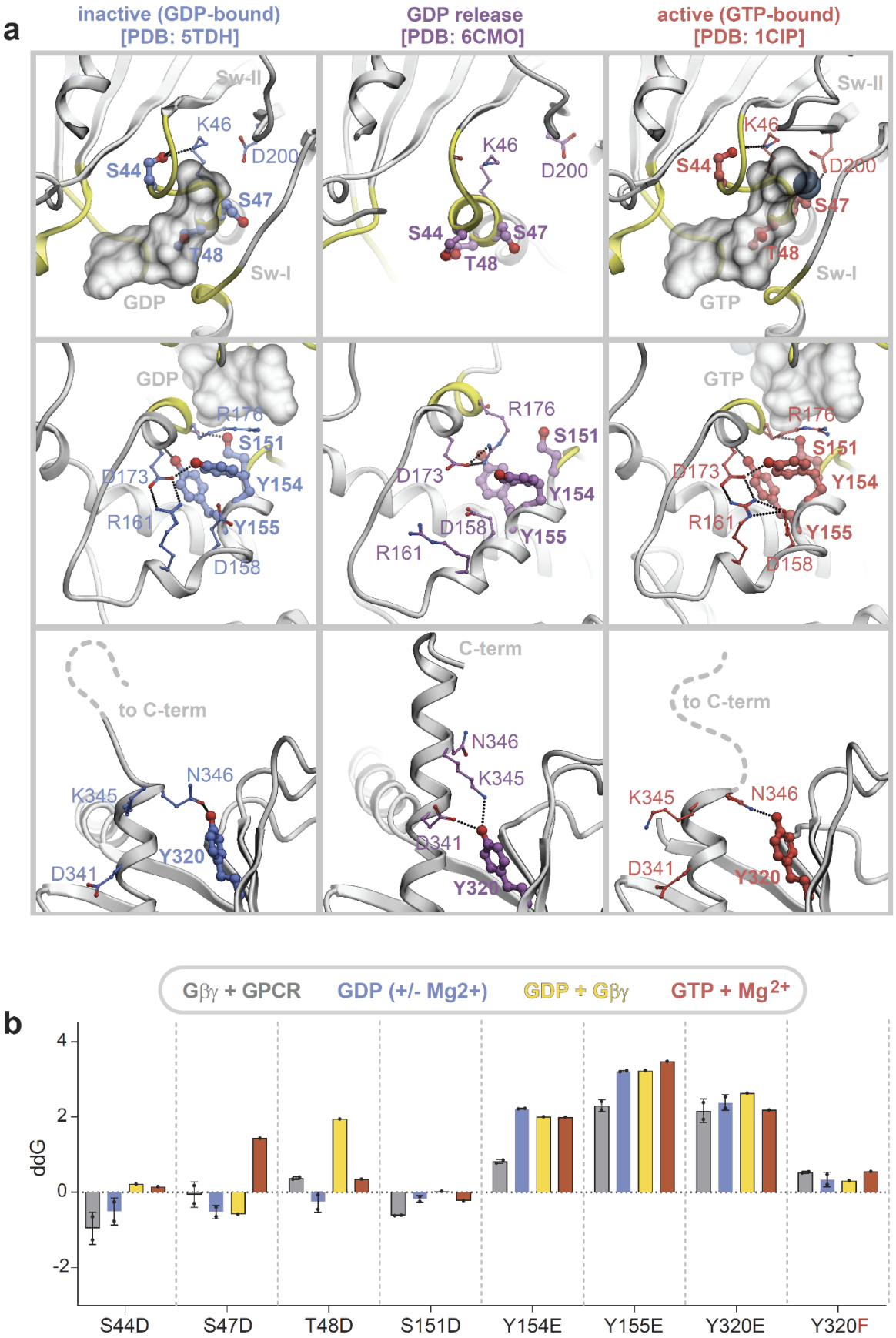

Figure 6: **Computational prediction of the impact of residue mutation on the stability of Gαi in various complexes**.

a. Crystal structure of WT Gαi3, highlighting contact of the residues in the P-loop region (*Top panels*: S44, S47 and T48), interdomain cleft (*Middle*: Y154 and Y155) and the C terminal α5 helix region packed against β4-β6 sheets (*Bottom panels*: Y320), in their GDP and Gβγ-bound inactive state (PDB: TDH), GDP release state (PDB: 6CMO) and GTP-bound active state (PDB:1CIP). H-bonds between the residues which were used in this study and its neighboring residues in the non-phosphorylated state.

b. Bar graph displays the computationally predicted effects of phosphomimicking or non-phosphorylatable mutations on the stability of Gαi3 in various complexes and conformations, including a complex with Gβγ+GPCR (PDB:6cmo,6ot0), GDP (+/-Mg^{2+}; PDB:1bof, 1gdd), GDP+Gβγ (PDB:1gg2), GTP+Mg^{2+} (PDB:1gia). Bar height indicates delta delta G [ddG], i.e., the predicted change in the change in Gibbs free energy of folding; higher / more positive bars reflect a larger degree of destabilization by the respective mutation while negative numbers indicate the opposite. See **Supplementary Figure 4a** for the relative stability of the different mutant state conformations and complex compositions compared to the Gβγ-bound state, and **Supplementary Figure 4b** for the extended analysis of both non-phosphorylatable substitutions (Ala, Phe) as well as phosphomimicking substitutions at each site.

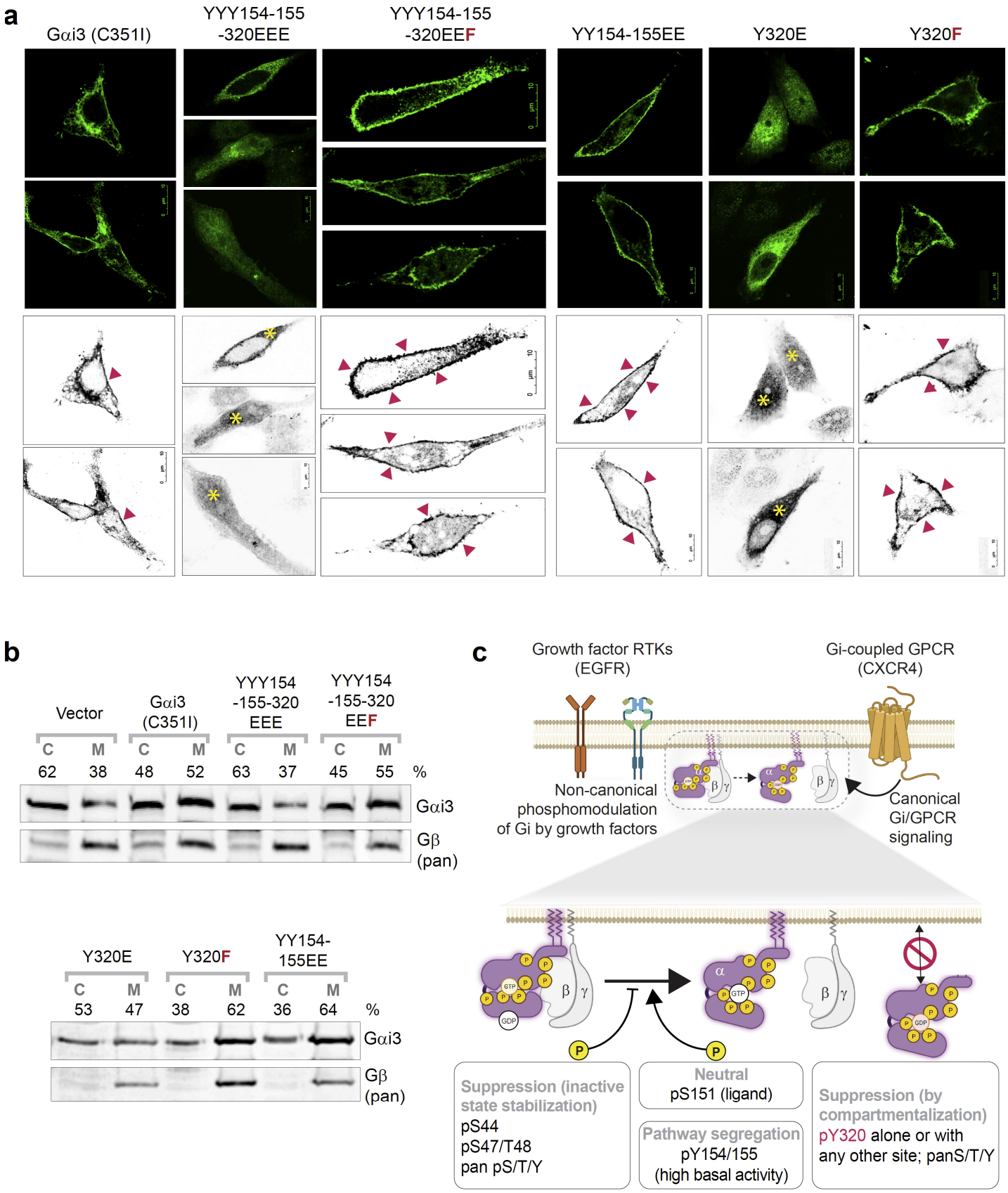

Figure 7: **Effect of phosphomimicking or non-phosphorylatable Gαi3 mutants on protein localization.**

a. The subcellular localization of the indicated Gαi3 constructs was assessed in transiently expressing HeLa cells by confocal immunofluorescence microscopy. Representative images are displayed as assembled montage in panel a. *Upper panels*: green, Gαi3; blue, nucleus/DAP). *Lower panels*: green channels depicting Gαi3 alone are presented in grayscale (red arrowheads, peripheral membrane localization; yellow asterisks, intracellular localization). Scale bars: 10 μm.

b. Membrane localization of the indicated Gαi3 constructs and pan-Gβ were assessed by subcellular fractionation of post-nuclear supernatants derived from the homogenates of each transiently expressing HeLa cell line in panel a. Immunoblots representative of 3 independent biological repeats are shown. C, cytosol; M, crude membranes. Numbers represent % distribution of Gαi3 protein in equivalent portions of cytosol and membrane fractions (10% of each fraction), as determined by quantitative immunoblotting (see *Methods*).

c. Schematic summarizes the key findings in this work. Growth factors may have at least 3 distinct effects on canonical Gα(i)βγ/GPCR signaling via phosphorylation of Gαi. Phosphorylation of some clusters of residues may suppress signaling by stabilizing the GDP-bound conformation (S44) or stabilizing the GDP/Gβγ-bound state (S47/T48) and thereby impeding ligand-stimulated nucleotide exchange and trimer dissociation (S44, S47, and T48). Phosphorylation at other sites may either have no effect (S151) or result in a segregation (Y154, Y155) between non-canonical (GF-RTK→Gi) and canonical (Gi/GPCR) pathways, while maintaining high basal activity due to defective Gβγ sequestration. Finally, phosphorylation at one key site may compartmentalize signaling via the regulation of G protein localization at the PM. See also **Table 3** for a comprehensive summary of all mutants tested in this work.

BIBLIOGRAPHY CITED:

1. G. Vert, J. Chory, Crosstalk in cellular signaling: background noise or the real thing? *Developmental cell* **21**, 985-991 (2011); published online EpubDec 13 (10.1016/j.devcel.2011.11.006).
2. J. S. Logue, D. K. Morrison, Complexity in the signaling network: insights from the use of targeted inhibitors in cancer therapy. *Genes & development* **26**, 641-650 (2012); published online EpubApr 1 (10.1101/gad.186965.112).
3. F. Siso-Nadal, J. J. Fox, S. A. Laporte, T. E. Hébert, P. S. Swain, Cross-talk between signaling pathways can generate robust oscillations in calcium and cAMP. *PloS one* **4**, e7189 (2009); published online EpubOct 21 (10.1371/journal.pone.0007189).
4. S. Tsunoda, J. Sierralta, C. S. Zuker, Specificity in signaling pathways: assembly into multimolecular signaling complexes. *Current opinion in genetics & development* **8**, 419-422 (1998); published online EpubAug (10.1016/s0959-437x(98)80112-3).
5. N. A. Kalogriopoulos, I. Lopez-Sanchez, C. Lin, T. Ngo, K. K. Midde, S. Roy, N. Aznar, F. Murray, M. Garcia-Marcos, I. Kufareva, M. Ghassemian, P. Ghosh, Receptor tyrosine kinases activate heterotrimeric G proteins via phosphorylation within the interdomain cleft of Gαi. **117**, 28763-28774 (2020)doi:10.1073/pnas.2004699117).
6. A. Bennasroune, A. Gardin, D. Aunis, G. Crémel, P. Hubert, Tyrosine kinase receptors as attractive targets of cancer therapy. *Critical Reviews in Oncology/Hematology* **50**, 23-38 (2004); published online Epub2004/04/01/ (https://doi.org/10.1016/j.critrevonc.2003.08.004).
7. A. G. Gilman, G proteins: transducers of receptor-generated signals. *Annual review of biochemistry* **56**, 615-649 (1987)10.1146/annurev.bi.56.070187.003151).
8. A. J. Morris, C. C. Malbon, Physiological regulation of G protein-linked signaling. *Physiological reviews* **79**, 1373-1430 (1999); published online EpubOct (10.1152/physrev.1999.79.4.1373).
9. V. L. Lowes, N. Y. Ip, Y. H. Wong, Integration of signals from receptor tyrosine kinases and g protein-coupled receptors. *Neuro-Signals* **11**, 5-19 (2002); published online EpubJan-Feb (10.1159/000057317).
10. A. Piiper, S. Zeuzem, Receptor tyrosine kinases are signaling intermediates of G protein-coupled receptors. *Curr Pharm Des* **10**, 3539-3545 (2004); published online Epub2004 (10.2174/1381612043382936).
11. K. Natarajan, B. C. Berk, Crosstalk coregulation mechanisms of G protein-coupled receptors and receptor tyrosine kinases. *Methods in molecular biology (Clifton, N.J.)* **332**, 51-77 (2006)10.1385/1-59745-048-0:51).
12. B. H. Shah, K. J. Catt, GPCR-mediated transactivation of RTKs in the CNS: mechanisms and consequences. *Trends in neurosciences* **27**, 48-53 (2004); published online EpubJan (10.1016/j.tins.2003.11.003).
13. V. Di Liberto, G. Mudò, N. Belluardo, Crosstalk between receptor tyrosine kinases (RTKs) and G protein-coupled receptors (GPCR) in the brain: Focus on heteroreceptor complexes and related functional neurotrophic effects. *Neuropharmacology* **152**, 67-77 (2019); published online EpubJul 1 (10.1016/j.neuropharm.2018.11.018).
14. H. Daub, F. U. Weiss, C. Wallasch, A. Ullrich, Role of transactivation of the EGF receptor in signalling by G-protein-coupled receptors. *Nature* **379**, 557-560 (1996); published online EpubFeb 8 (10.1038/379557a0).
15. L. M. Luttrell, Y. Daaka, R. J. Lefkowitz, Regulation of tyrosine kinase cascades by G-protein-coupled receptors. *Curr Opin Cell Biol* **11**, 177-183 (1999); published online EpubApr (10.1016/s0955-0674(99)80023-4).
16. B. Schäfer, A. Gschwind, A. Ullrich, Multiple G-protein-coupled receptor signals converge on the epidermal growth factor receptor to promote migration and invasion. *Oncogene* **23**, 991-999 (2004); published online EpubJan 29 (10.1038/sj.onc.1207278).
17. H. Ohtsu, P. J. Dempsey, S. Eguchi, ADAMs as mediators of EGF receptor transactivation by G protein-coupled receptors. *American journal of physiology. Cell physiology* **291**, C1-10 (2006); published online EpubJul (10.1152/ajpcell.00620.2005).

18. N. Prenzel, E. Zwick, H. Daub, M. Leserer, R. Abraham, C. Wallasch, A. Ullrich, EGF receptor transactivation by G-protein-coupled receptors requires metalloproteinase cleavage of proHB-EGF. *Nature* **402**, 884-888 (1999); published online EpubDec 23-30 (10.1038/47260).
19. D. Guidolin, L. F. Agnati, M. Marcoli, D. O. Borroto-Escuela, K. Fuxe, G-protein-coupled receptor type A heteromers as an emerging therapeutic target. *Expert opinion on therapeutic targets* **19**, 265-283 (2015); published online EpubFeb (10.1517/14728222.2014.981155).
20. H. Sun, J. M. Seyer, T. B. Patel, A region in the cytosolic domain of the epidermal growth factor receptor antithetically regulates the stimulatory and inhibitory guanine nucleotide-binding regulatory proteins of adenylyl cyclase. **92**, 2229-2233 (1995)doi:10.1073/pnas.92.6.2229).
21. H. Poppleton, H. Sun, D. Fulgham, P. Bertics, T. B. Patel, Activation of Gsalpha by the epidermal growth factor receptor involves phosphorylation. *J Biol Chem* **271**, 6947-6951 (1996); published online EpubMar 22 (10.1074/jbc.271.12.6947).
22. C. Marty, R. D. Ye, Heterotrimeric G protein signaling outside the realm of seven transmembrane domain receptors. *Molecular pharmacology* **78**, 12-18 (2010); published online EpubJul (10.1124/mol.110.063453).
23. B. G. Nair, B. Parikh, G. Milligan, T. B. Patel, Gs alpha mediates epidermal growth factor-elicited stimulation of rat cardiac adenylate cyclase. *J Biol Chem* **265**, 21317-21322 (1990); published online EpubDec 5 (
24. H. Sun, Z. Chen, H. Poppleton, K. Scholich, J. Mullenix, G. J. Weipz, D. L. Fulgham, P. J. Bertics, T. B. Patel, The juxtamembrane, cytosolic region of the epidermal growth factor receptor is involved in association with alpha-subunit of Gs. *J Biol Chem* **272**, 5413-5420 (1997); published online EpubFeb 28 (
25. Y. Zick, R. Sagi-Eisenberg, M. Pines, P. Gierschik, A. M. Spiegel, Multisite phosphorylation of the alpha subunit of transducin by the insulin receptor kinase and protein kinase C. *Proc Natl Acad Sci U S A* **83**, 9294-9297 (1986); published online EpubDec (10.1073/pnas.83.24.9294).
26. J. Krupinski, R. Rajaram, M. Lakonishok, J. L. Benovic, R. A. Cerione, Insulin-dependent phosphorylation of GTP-binding proteins in phospholipid vesicles. *Journal of Biological Chemistry* **263**, 12333-12341 (1988)10.1016/S0021-9258(18)37759-7).
27. W. P. Hausdorff, J. A. Pitcher, D. K. Luttrell, M. E. Linder, H. Kurose, S. J. Parsons, M. G. Caron, R. J. Lefkowitz, Tyrosine phosphorylation of G protein alpha subunits by pp60c-src. *Proc Natl Acad Sci U S A* **89**, 5720-5724 (1992); published online EpubJul 1 (10.1073/pnas.89.13.5720).
28. H. Umemori, T. Inoue, S. Kume, N. Sekiyama, M. Nagao, H. Itoh, S. Nakanishi, K. Mikoshiba, T. Yamamoto, Activation of the G protein Gq/11 through tyrosine phosphorylation of the alpha subunit. *Science* **276**, 1878-1881 (1997); published online EpubJun 20 (10.1126/science.276.5320.1878).
29. P. Ghosh, M. Mullick, Building unconventional G protein-coupled receptors, one block at a time. *Trends Pharmacol Sci* **42**, 514-517 (2021); published online EpubJul (10.1016/j.tips.2021.04.005).
30. M. Neves, C. Perpiñá-Viciano, P. Penela, C. Hoffmann, F. Mayor, Jr., Modulation of CXCR4-Mediated Gi1 Activation by EGF Receptor and GRK2. *ACS Pharmacol Transl Sci* **3**, 627-634 (2020); published online EpubAug 14 (10.1021/acsptsci.0c00021).
31. D. J. Douglas, A. J. Frank, D. Mao, Linear ion traps in mass spectrometry. *Mass spectrometry reviews* **24**, 1-29 (2005); published online EpubJan-Feb (10.1002/mas.20004).
32. N. E. Bhola, J. R. Grandis, Crosstalk between G-protein-coupled receptors and epidermal growth factor receptor in cancer. *Frontiers in bioscience : a journal and virtual library* **13**, 1857-1865 (2008); published online EpubJan 1 (10.2741/2805).
33. L. E. Kilpatrick, S. J. Hill, Transactivation of G protein-coupled receptors (GPCRs) and receptor tyrosine kinases (RTKs): Recent insights using luminescence and fluorescence technologies. *Current Opinion in Endocrine and Metabolic Research* **16**, 102-112 (2021); published online Epub2021/02/01/ (https://doi.org/10.1016/j.coemr.2020.10.003).
34. K. Oda, Y. Matsuoka, A. Funahashi, H. Kitano, A comprehensive pathway map of epidermal growth factor receptor signaling. **1**, 2005.0010 (2005)https://doi.org/10.1038/msb4100014).
35. D. Sun, T. Flock, X. Deupi, S. Maeda, M. Matkovic, S. Mendieta, D. Mayer, R. Dawson, G. F. X. Schertler, M. Madan Babu, D. B. Veprintsev, Probing Gαi1 protein activation at single-amino acid resolution. *Nat Struct Mol Biol* **22**, 686-694 (2015); published online EpubSep (10.1038/nsmb.3070).

36. M. N. Liang, J. C. Garrison, The epidermal growth factor receptor is coupled to a pertussis toxin-sensitive guanine nucleotide regulatory protein in rat hepatocytes. *Journal of Biological Chemistry* **266**, 13342-13349 (1991); published online Epub1991/07/15/ (https://doi.org/10.1016/S0021-9258(18)98845-9).
37. R. M. O'Brien, M. D. Houslay, G. Milligan, K. Siddle, The insulin receptor tyrosyl kinase phosphorylates holomeric forms of the guanine nucleotide regulatory proteins Gi and Go. *FEBS letters* **212**, 281-288 (1987); published online EpubFeb 23 (10.1016/0014-5793(87)81361-3).
38. D. J. Carty, Pertussis toxin-catalyzed ADP-ribosylation of G proteins. *Methods Enzymol* **237**, 63-70 (1994)10.1016/s0076-6879(94)37053-2).
39. S. Mangmool, H. Kurose, G(i/o) protein-dependent and -independent actions of Pertussis Toxin (PTX). *Toxins* **3**, 884-899 (2011); published online EpubJul (10.3390/toxins3070884).
40. J. M. Busillo, J. L. Benovic, Regulation of CXCR4 signaling. *Biochimica et biophysica acta* **1768**, 952-963 (2007); published online EpubApr (10.1016/j.bbamem.2006.11.002).
41. Y. Cheng, X. Che, S. Zhang, T. Guo, X. He, Y. Liu, X. Qu, Positive Cross-Talk Between CXC Chemokine Receptor 4 (CXCR4) and Epidermal Growth Factor Receptor (EGFR) Promotes Gastric Cancer Metastasis via the Nuclear Factor kappa B (NF-kB)-Dependent Pathway. *Medical science monitor : international medical journal of experimental and clinical research* **26**, e925019 (2020); published online EpubSep 3 (10.12659/msm.925019).
42. C. Wang, H. Cheng, Y. Li, Role of SDF-1 and CXCR4 in the proliferation, migration and invasion of cervical cancer. *Pakistan journal of pharmaceutical sciences* **29**, 2151-2154 (2016); published online EpubNov (
43. K. A. Martemyanov, Mechanisms of Gβγ Release upon GPCR Activation. *Trends Biochem Sci* **46**, 703-704 (2021); published online EpubSep (10.1016/j.tibs.2021.05.002).
44. F. Bachelerie, A. Ben-Baruch, A. M. Burkhardt, C. Combadiere, J. M. Farber, G. J. Graham, R. Horuk, A. H. Sparre-Ulrich, M. Locati, A. D. Luster, A. Mantovani, K. Matsushima, P. M. Murphy, R. Nibbs, H. Nomiyama, C. A. Power, A. E. Proudfoot, M. M. Rosenkilde, A. Rot, S. Sozzani, M. Thelen, O. Yoshie, A. Zlotnik, International Union of Basic and Clinical Pharmacology. [corrected]. LXXXIX. Update on the extended family of chemokine receptors and introducing a new nomenclature for atypical chemokine receptors. *Pharmacological reviews* **66**, 1-79 (2014)10.1124/pr.113.007724).
45. C. J. Draper-Joyce, M. Khoshouei, D. M. Thal, Y.-L. Liang, A. T. N. Nguyen, S. G. B. Furness, H. Venugopal, J.-A. Baltos, J. M. Plitzko, R. Danev, W. Baumeister, L. T. May, D. Wootten, P. M. Sexton, A. Glukhova, A. Christopoulos, Structure of the adenosine-bound human adenosine A1 receptor–Gi complex. *Nature* **558**, 559-563 (2018); published online Epub2018/06/01 (10.1038/s41586-018-0236-6).
46. Y. L. Liang, P. Zhao, C. Draper-Joyce, J. A. Baltos, A. Glukhova, T. T. Truong, L. T. May, A. Christopoulos, D. Wootten, P. M. Sexton, S. G. B. Furness, Dominant Negative G Proteins Enhance Formation and Purification of Agonist-GPCR-G Protein Complexes for Structure Determination. *ACS Pharmacol Transl Sci* **1**, 12-20 (2018); published online EpubSep 14 (10.1021/acsptsci.8b00017).
47. X. Qi, H. Liu, B. Thompson, J. McDonald, C. Zhang, X. Li, Cryo-EM structure of oxysterol-bound human Smoothened coupled to a heterotrimeric Gi. *Nature* **571**, 279-283 (2019); published online Epub2019/07/01 (10.1038/s41586-019-1286-0).
48. P. M. Murphy, M. Baggiolini, I. F. Charo, C. A. Hébert, R. Horuk, K. Matsushima, L. H. Miller, J. J. Oppenheim, C. A. Power, International union of pharmacology. XXII. Nomenclature for chemokine receptors. *Pharmacological reviews* **52**, 145-176 (2000); published online EpubMar (
49. L. I. Jiang, J. Collins, R. Davis, K. M. Lin, D. DeCamp, T. Roach, R. Hsueh, R. A. Rebres, E. M. Ross, R. Taussig, I. Fraser, P. C. Sternweis, Use of a cAMP BRET sensor to characterize a novel regulation of cAMP by the sphingosine 1-phosphate/G13 pathway. *J Biol Chem* **282**, 10576-10584 (2007); published online EpubApr 6 (10.1074/jbc.M609695200).
50. Q. Wan, N. Okashah, A. Inoue, R. Nehmé, B. Carpenter, C. G. Tate, N. A. Lambert, Mini G protein probes for active G protein-coupled receptors (GPCRs) in live cells. *J Biol Chem* **293**, 7466-7473 (2018); published online EpubMay 11 (10.1074/jbc.RA118.001975).
51. C. Akekawatchai, J. D. Holland, M. Kochetkova, J. C. Wallace, S. R. McColl, Transactivation of CXCR4 by the insulin-like growth factor-1 receptor (IGF-1R) in human MDA-MB-231 breast cancer epithelial cells. *J Biol Chem* **280**, 39701-39708 (2005); published online EpubDec 2 (10.1074/jbc.M509829200).

52. P. Dillenburg-Pilla, V. Patel, C. M. Mikelis, C. R. Zarate-Blades, C. L. Doci, P. Amornphimoltham, Z. Wang, D. Martin, K. Leelahavanichkul, R. T. Dorsam, A. Masedunskas, R. Weigert, A. A. Molinolo, J. S. Gutkind, SDF-1/CXCL12 induces directional cell migration and spontaneous metastasis via a CXCR4/Galphai/mTORC1 axis. *FASEB J* **29**, 1056-1068 (2015); published online EpubMar (10.1096/fj.14-260083).
53. S. J. Wright, R. Inchausti, C. J. Eaton, S. Krystofova, K. A. Borkovich, RIC8 is a guanine-nucleotide exchange factor for Galpha subunits that regulates growth and development in Neurospora crassa. *Genetics* **189**, 165-176 (2011); published online EpubSep (10.1534/genetics.111.129270).
54. L. J. McClelland, K. Zhang, T.-C. Mou, J. Johnston, C. Yates-Hansen, S. Li, C. J. Thomas, T. I. Doukov, S. Triest, A. Wohlkonig, G. G. Tall, J. Steyaert, W. Chiu, S. R. Sprang, Structure of the G protein chaperone and guanine nucleotide exchange factor Ric-8A bound to Gαi1. *Nature Communications* **11**, 1077 (2020); published online Epub2020/02/26 (10.1038/s41467-020-14943-4).
55. R. O. Dror, T. J. Mildorf, D. Hilger, A. Manglik, D. W. Borhani, D. H. Arlow, A. Philippsen, N. Villanueva, Z. Yang, M. T. Lerch, W. L. Hubbell, B. K. Kobilka, R. K. Sunahara, D. E. Shaw, SIGNAL TRANSDUCTION. Structural basis for nucleotide exchange in heterotrimeric G proteins. *Science* **348**, 1361-1365 (2015); published online EpubJun 19 (10.1126/science.aaa5264).
56. N. A. Kalogriopoulos, S. D. Rees, T. Ngo, N. J. Kopcho, A. V. Ilatovskiy, N. Sun, E. A. Komives, G. Chang, P. Ghosh, I. Kufareva, Structural basis for GPCR-independent activation of heterotrimeric Gi proteins. **116**, 16394-16403 (2019)doi:10.1073/pnas.1906658116).
57. S. R. Sprang, Invited review: Activation of G proteins by GTP and the mechanism of Galpha-catalyzed GTP hydrolysis. *Biopolymers* **105**, 449-462 (2016); published online EpubAug (10.1002/bip.22836).
58. M. Saraste, P. R. Sibbald, A. Wittinghofer, The P-loop — a common motif in ATP- and GTP-binding proteins. *Trends in Biochemical Sciences* **15**, 430-434 (1990); published online Epub1990/11/01/ (https://doi.org/10.1016/0968-0004(90)90281-F).
59. J. Chu, H. Zheng, Y. Zhang, H. H. Loh, P. Y. Law, Agonist-dependent mu-opioid receptor signaling can lead to heterologous desensitization. *Cell Signal* **22**, 684-696 (2010); published online EpubApr (10.1016/j.cellsig.2009.12.003).
60. A. Marivin, A. Leyme, K. Parag-Sharma, V. DiGiacomo, A. Y. Cheung, L. T. Nguyen, I. Dominguez, M. Garcia-Marcos, Dominant-negative Galpha subunits are a mechanism of dysregulated heterotrimeric G protein signaling in human disease. *Science signaling* **9**, ra37 (2016); published online EpubApr 12 (10.1126/scisignal.aad2429).
61. L. Navarro, A. Koller, R. Nordfelth, H. Wolf-Watz, S. Taylor, J. E. Dixon, Identification of a molecular target for the Yersinia protein kinase A. *Mol Cell* **26**, 465-477 (2007); published online EpubMay 25 (10.1016/j.molcel.2007.04.025).
62. K. Afshar, F. S. Willard, K. Colombo, D. P. Siderovski, P. Gönczy, Cortical localization of the Gα protein GPA-16 requires RIC-8 function during C. elegans asymmetric cell division. *Development* **132**, 4449-4459 (2005)10.1242/dev.02039 %J Development).
63. N. B. David, C. A. Martin, M. Segalen, F. Rosenfeld, F. Schweisguth, Y. Bellaïche, Drosophila Ric-8 regulates Gαi cortical localization to promote Gαi-dependent planar orientation of the mitotic spindle during asymmetric cell division. *Nature Cell Biology* **7**, 1083-1090 (2005); published online Epub2005/11/01 (10.1038/ncb1319).
64. M. Gabay, M. E. Pinter, F. A. Wright, P. Chan, A. J. Murphy, D. M. Valenzuela, G. D. Yancopoulos, G. G. Tall, Ric-8 Proteins Are Molecular Chaperones That Direct Nascent G Protein α Subunit Membrane Association. **4**, ra79-ra79 (2011)doi:10.1126/scisignal.2002223).
65. B. Hampoelz, O. Hoeller, S. K. Bowman, D. Dunican, J. A. Knoblich, Drosophila Ric-8 is essential for plasma-membrane localization of heterotrimeric G proteins. *Nature Cell Biology* **7**, 1099-1105 (2005); published online Epub2005/11/01 (10.1038/ncb1318).
66. H. Wang, K. H. Ng, H. Qian, D. P. Siderovski, W. Chia, F. Yu, Ric-8 controls Drosophila neural progenitor asymmetric division by regulating heterotrimeric G proteins. *Nat Cell Biol* **7**, 1091-1098 (2005); published online EpubNov (10.1038/ncb1317).